LMS registration of rigid transformations

C Smith, D R Campbell

Dept Electrical & Electronic Engineering, University of Paisley, High Street, Paisley PA1 2BE
Tel: +44 0141 848 3428 Fax: +44 0141 848 3404 Email:cameron.smith@paisley.ac.uk

Abstract
Methods are investigated to improve the registration of images corrupted by rigid displacements using the Least Mean Square (LMS) algorithm. Results show that LMS adaptive registration (LMSAR) is effective for small translational displacements, but fails for large translational displacements where the correlation between the rotation data sets is too weak. In an attempt to improve the robustness of LMSAR, various methods are investigated and a modified LMSAR technique is introduced. The modified LMSAR is compared with the Fourier Shift Theorem (FST) for clean and noisy images where the LMSAR accuracy is similar to the FST for clean image. As expected the LMSAR appears more susceptible to noise, but the LMSAR offers reduced computation over the FST for circumstances involving searches over a large angular range.

1. Introduction

Image registration is primarily concerned with the alignment of image features, or primitives, in two images. It has become an important area for machine vision and image processing research during the last decade and is required in many areas including remote sensing, medical scanner and military applications [1]. The most common registration problems can be categorized by transformations, such as rigid, affine, perspective, and polynomial, where the misregistrations can be further categorized as global or local. The tools used to tackle the rigid transformation problem are amongst the most basic and are frequently used for simple registration problems. Rigid transformations consist of translational displacement (TD) and rotation. This paper presents an adaptive solution to the registration of rigid transformations.

Current techniques available include cross–correlation, template matching, and Fourier methods [2]. Cross–correlation and template matching are computationally intensive where all possible translations, rotations and scaling have to be implemented, thus Fourier methods are often favoured. The heart of the Fourier methods is the Fourier Shift Theorem (FST) relating the phase of the cross–power spectrum to the displacement between two images. Castro and Morandi [3] described a method to correct both translation and rotation between two images using the FST, and this is used here as a benchmark to test the new LMS registration approach.

An adaptive method employing the LMS algorithm [4] was presented by Smith and Campbell [5] to register rotated images. This method consists of two components: firstly locating the centre of rotation (COR) between the two images, and secondly using the LMS algorithm to minimise the error between data sequences extracted from the two images. The rotation is determined from the position of the largest converged filter coefficient and it was shown that the LMS algorithm was as effective as the FST for registering rotation given the correct location for the COR. The location of the COR however was often not sufficiently accurate to ensure correct estimation of rotation. This work has been expanded to develop an adaptive solution that registers both translational and rotational displacements ie. rigid transformations, and does not require ‘a priori’ information regarding the COR location.

2. LMS adaptive registration

Translational displacement can be found using the TDLMS algorithm [6] by examining the weight coefficients after convergence where the location of the largest weight coefficient represents the translational displacement. Rotation can similarly be found by using an LMS algorithm on a set of data obtained through sampling at a fixed radius through 360 degrees [5]. When both TD and rotation are present, the correlation for both the TD data pair and rotation data pair is weakened.
Simultaneous estimation of translation and rotation using LMS adaptive registration (LMSAR) is described here, where adjustments are made to the misregistered image at set intervals during the process (Figure 1). The TD is determined from a finite window placed in the centre of each image to reduce the effect of rotation, and rotation is estimated by processing data obtained by mapping the rotation to a translation about the image centre using the average pixel intensity I_{ave} across a radial scan r_{min} to r_{min+n}.

$$I_{ave}(\theta) = \frac{1}{n+1}\sum_{i=0}^{n} I(r_{min+i}, \theta) \qquad (1)$$

During the first update to the misregistered image, if the rotation exceeds a preset threshold the TD is not corrected, otherwise the translational displacement detected is compared against a TD threshold. If the TD detected exceeds the threshold it is re–determined using a larger filter, where if the same result is returned using a larger filter both translational displacement and rotation are corrected, otherwise rotation alone is corrected. Table 1 shows the results of applying LMS adaptive registration to displaced copies of 'Lenna' (Figure 2) where 20 sweeps over the misregistered image were made, corresponding to four updates. With a rotation of 40° displaced by a TD of 1,5 the detected TD was 4,3, which is correct as the TD was rotated during the first update. For larger TDs, errors in the rotation estimate were introduced in the 1st estimate and propagated through further updates to the final result. Local averaging to increase correlation is investigated in the next section to try and make the rotation estimate more accurate.

TD (row,col)	$Dist_{Eucl}$	θ	$TD_{detected}$	$\theta_{detected}$
1 down,5 right	5.099	0	1 down,5 right	0
1 down,5 right	5.099	40	4 down,3 right	39.375
0 down,0 right	0.000	40	0 down,0 right	39.375
5 down,5 right	7.071	0	6 down,6 right	0
5 down,5 right	7.071	40	6 down,1 right	36.5625

Table 1: Basic LMS adaptive registration of 'Lenna'

3. LMS adaptive registration modifications

The local averaging is described by

$$f_{avg}(x, y) = \frac{1}{n^2} \sum_{a=int(\frac{x}{n})}^{(int(\frac{x}{n})+1)*n} \sum_{a,b=int(\frac{y}{n})}^{(int(\frac{y}{n})+1)*n} f(a, b) \qquad (2)$$

where f is the image, n is the local area size, and int(m) takes the integer part of m. The location of the smallest mse within a $\pm 50^\circ$ range was examined for test images 'Lenna', 'Trinity' and 'Salonika' displaced by 40° rotation and TDs of up to 20 rows by 20 columns. A local area $n < 8$ made no difference to the minimum mse location; n=8,16 moved the location of the minimum mse closer to the true rotation, but only by one or two samples (2.8125° angular step size for this test); the averaging effect of n>16 was found to introduce unacceptable errors. If the rotation is not a multiple of the angular step size there will be a maximum error of ±0.5*angular step size. If the angular sampling rate is increased, the rotation estimate error is reduced due to smaller angular quantisation.

It has been observed that with data which has been translated and rotated the LMS algorithm does not always converge to the smallest mse location. A variable step–size LMS algorithm [7] was investigated but at present no improvement in accuracy has been found.

The LMSAR was modified for the later test by: 1) Estimating the initial rotation using a local average over 16 by 16 pixel blocks; 2) Correcting TD alone in the second update if it had not been corrected in the first since the TD estimate will be more accurate due to smaller rotation, while the rotation estimate will still be vulnerable due to TD.

4. Fourier Shift Theorem

If $g(x+\Delta x,y+\Delta y)$ is a displaced copy of f(x,y) of Δx rows and Δy columns, their Fourier transforms are related by

$$F(w_x, w_y) = G(w_{x,} w_y) e^{-j(w_x \Delta x + w_y \Delta y)} \qquad (3)$$

Both images have the same Fourier magnitude, with only the phase changing. This change in phase is directly proportional to the translational displacement, and is the basis for the Fourier Shift Theorem (FST) [2].

$$\frac{F(w_x, w_y) G^*(w_x, w_y)}{|F(w_x, w_y) G^*(w_x, w_y)|} = e^{(w_x \Delta x + w_y \Delta y)} \qquad (4)$$

Equation (4) shows the calculation of the cross–power spectrum phase where G^* is the complex conjugate of G. If the inverse Fourier transform of this phase is taken, the result will be an image that is approximately zero everywhere except at the location of the displacement, which is an impulse. De Castro proposed a two–stage approach to registering images that contain both translational displacement and rotation [3]. If the phase of the cross–power spectrum is calculated as a function of angular rotation ϕ, and using polar co–ordinates for simplicity, equation (4) becomes

$$\frac{F(r, \theta) G^*(r, \theta - \phi)}{|F(r, \theta) G^*(r, \theta - \phi)|} = H(r, \theta; \phi) \qquad (5)$$

From equation (5), if an accurate estimate is made of the rotation ϕ, then the function H reduces to that of equation (4). De Castro adjusts the angle ϕ, where for each adjustment the inverse Fourier transform of H(.) is determined. The angle that returns the largest impulse response in the spatial domain is accepted as the angle of rotation between the two images, and the peak location identifies the TD.

5. Experimental results

'Lenna', 'Trinity', 'Salonika' and 'Turing' are rotated by 40° and displaced by various translational displacements (Fig 2). The modified LMSAR and the FST are applied to the misregistered images for clean and noisy environments, where additive Gaussian noise of variance 900 was used for the noisy case. The angular range searched by both the FST and modified LMSAR was $\pm 50^\circ$, and a 41*41 filter was used in the LMSAR translation estimate for images of shifts 5*5 and 10*10, while a 61*61 filter was used for shifts 20 by 20. For the 61*61 filter, the image area over which it was moved had to be enlarged to allow a sufficient number of iterations. Table 2 shows the results, where the rotation was corrected about the image centre before correcting the TD. Due to the order of corrections, the TD present after the correction of rotation is 7 rows down, 1 cols right (5 by 5); 14 rows down, 1 col right (10 by 10); 28 rows down 2 cols right (20 by 20). The TD quoted for the modified LMSAR in table 2 does not take account of rotational adjustments beyond the second

(a) 'Lenna'

(b) 'Trinity'

(c) 'Salonika'

(d) 'Turing'

Figure 2 – Test images

update, resulting in small errors.

The FST identifies the correct displacement for all clean images, while the modified LMSAR returns answers similar to the FST, although there are errors for some images for both rotation and TD estimates using the modified LMSAR ($\pm 1^{\circ}$, ±1 row/column). When registering noisy images, both modified LMSAR and FST are affected, however the modified LMSAR is shown to be more susceptible to noise than the FST. This is clearly seen for the noisy 'Turing' image displaced by 5 rows and 5 columns where the modified LMSAR has an error of 0 row 2 columns and -5° compared to 1 row 1 column and -1° for the FST. This was expected, since for large levels of noise the LMS algorithm will reduce the mse by filtering the noise rather than registering the images.

6. Conclusion

The modified LMSAR has been compared against the FST registering clean and noisy images. The order of filter used in the LMSAR is a trade–off between accuracy and complexity. For clean images the modified LMSAR accuracy is similar to the FST accuracy for most images used and had small errors for others, but for a TD of 20 pixels by 20 pixels the LMSAR failed to consistently identify the correct displacement, thus at present is only applicable to problems containing small TDs. In a noisy environment the modified LMSAR exhibits larger errors than the FST. Further updates for LMSAR when processing both clean and noisy images may reduce the error. Further work will be carried out for situations when a large number of rotations have to be examined, where the LMSAR may require fewer computations than the FST since the latter performs an exhaustive search across all candidate rotations.

References

[1] Lisa Gottesfeld Brown , " A survey of Image registration techniques", ACM Computing Surveys Vol.24 No.4 December 1992 pp325–376.

[2] C D Kuglin, D C Hines, " The phase correlation image alignment method", International Conference on Cybernetics and Society 1975 pp163–165.

[3] E De Castro, C Morandi, " Registration of translated and rotated images using Finite Fourier transforms", IEEE Transactions on Pattern Analysis and Machine Intelligence Vol.9 No.5 September 1987 pp700–703.

[4] Bernard Widrow, John R.Glover Jr, John M. McCool, John Kaunitz, Charles S. Williams, Robert H. Hearn , James R. Zeidler , Eugene Dong Jr, and Robert C. Goodlin, " Adaptive Noise Cancelling: Principles and Applications.", Proceedings of the IEEE, Vol 63 No.12 1975 pp1692–1716.

[5] C Smith, D R Campbell, " Application of LMS algorithm to registration of rotated images", Proc International workshop on Medical and Biological Signal Processing 1995 pp41–46.

[6] Michael R Lynch and Peter J.W. Rayner , "A new approach to image registration utilising multidimensional LMS Adaptive filters" , IEEE International Conference on Acoustics, Speech, and Signal Processing 1988 pp920–923.

[7] R W Harris, D M Chabries, F A Bishop, "A variable step (VS) adaptive filter algorithm", IEEE Transactions on Acoustics, Speech and Signal Processing Vol.34 No.2 1986 pp309–316.

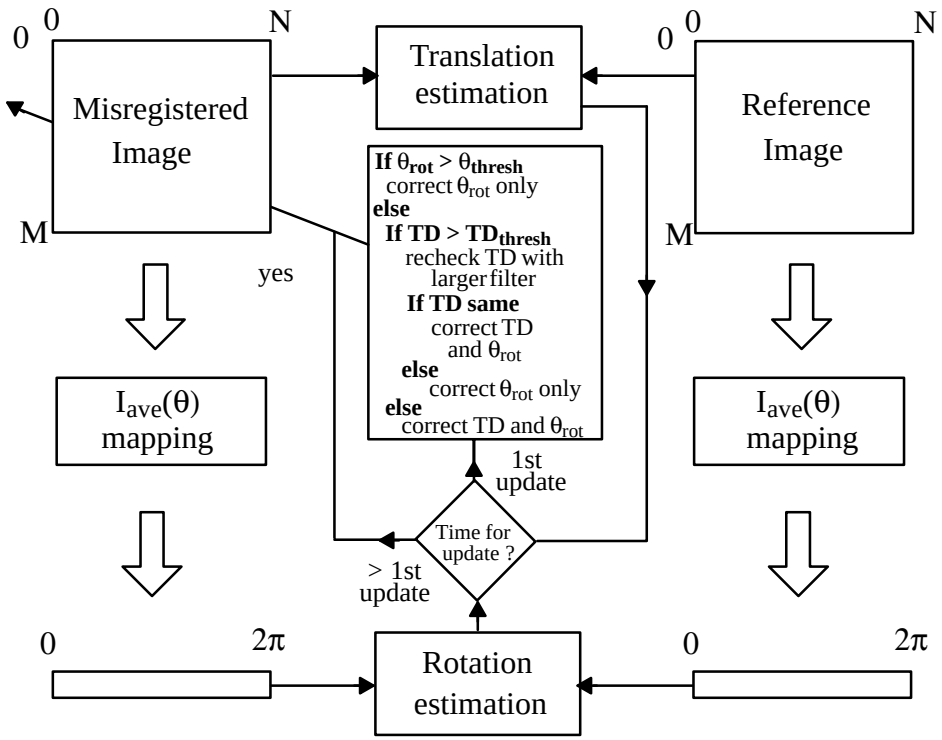

Figure 1 – LMS adaptive registration (LMSAR)

Image	Displacement		Clean: modified LMSAR		Clean: FST		SNR	Noisy ($\sigma_n^2 = 900$): modified LMSAR		Noisy ($\sigma_n^2 = 900$): FST	
	TD	θ	TD	θ	TD	θ		TD	θ	TD	θ
Lenna	5 rows down 5 cols right	40°	8 rows up 0 col left	–39°	7 rows up 1 col left	–40°	7.166	7 rows up 0 col left	–39°	7 rows up 1 col left	–40°
	10 rows down 10 cols right	40°	14 rows up 1 col right	–40°	14 rows up 1 col left	–40°	7.494	13 rows up 2 cols right	–40°	14 rows up 1 col left	–40°
	20 rows down 20 cols right	40°	28 rows up 2 cols left	–39°	28 rows up 2 cols left	–40°	8.188	28 rows up 3 cols right	–42°	28 rows up 2 cols left	–40°
Trinity	5 rows down 5 cols right	40°	7 rows up 0 col left	–40°	7 rows up 1 col left	–40°	5.387	7 rows up 0 col left	–40°	7 rows up 0 col left	–40°
	10 rows down 10 cols right	40°	14 rows up 1 col right	–40°	14 rows up 1 col left	–40°	5.294	14 rows up 1 col right	–40°	14 rows up 1 col left	–40°
	20 rows down 20 cols right	40°	28 rows up 3 cols right	–40°	28 rows up 2 cols left	–40°	5.146	28 rows up 2 cols right	–40°	28 rows up 2 cols left	–40°
Salonika	5 rows down 5 cols right	40°	7 rows up 1 col left	–40°	7 rows up 1 col left	–40°	9.794	7 rows up 1 col left	–39°	7 rows up 1 col left	–40°
	10 rows down 10 cols right	40°	14 rows up 4 cols left	–40°	14 rows up 1 col left	–40°	9.822	14 rows up 5 cols left	–40°	14 rows up 1 col left	–40°
	20 rows down 20 cols right	40°	29 rows up 3 cols right	–44°	28 rows up 2 cols left	–40°	9.871	29 rows up 3 cols right	–31°	28 rows up 2 cols left	–40°
Turing	5 rows down 5 cols right	40°	8 rows up 1 cols left	–39°	7 rows up 1 col left	–40°	1.782	7 rows up 3 cols left	–45°	8 rows up 0 col left	–41°
	10 rows down 10 cols right	40°	15 rows up 1 col left	–39°	14 rows up 1 col left	–40°	1.820	15 rows up 9 cols left	–43°	15 rows up 1 col left	–40°
	20 rows down 20 cols right	40°	27 rows up 10 cols left	–40°	28 rows up 2 cols left	–40°	1.903	27 rows up 11 cols left	–42°	28 rows up 4 cols left	–39°

Table 2 : Modified LMSAR Vs FST